# Particle-hole Symmetric Slave Boson Method for the Mixed Valence Problem

Liam L.H. Lau\* and Piers Coleman

Center for Materials Theory, Department of Physics and Astronomy,
Rutgers University, 136 Frelinghuysen Rd., Piscataway, NJ 08854-8019, USA

(Dated: August 26, 2025)

We introduce an analytic slave boson method for treating the finite U Anderson impurity model. Our approach introduces two bosons to track both  $Q \rightleftharpoons Q \pm 1$  valence fluctuations and reduces to a single symmetric s-boson in the effective action, encoding all the high energy atomic physics information in the boson's kinematics, while the low energy part of the action remains unchanged across finite U, infinite U, and Kondo limits. We recover the infinite U and Kondo limit actions from our approach and show that the Kondo resonance already develops in the normal state when the slave boson has yet to condense. We show that the slave rotor and s-boson have the same algebraic structure, and we establish a unified functional integral framework connecting the s-boson and slave rotor representations for the single impurity Anderson model.

#### I. INTRODUCTION

The single impurity Anderson model (SIAM) and its generalizations are foundational to our understanding of strongly correlated electron systems. The model describes tightly bound d-electrons that experience on-site Coulomb repulsion and hybridize with dispersive conduction c-electrons. This model captures the physics of local moment formation in metals with rare-earth magnetic impurities in both Kondo and mixed valence regimes and also underpins Dynamical Mean Field Theory (DMFT) [1-3] approach to strongly correlated electron systems, which maps the original lattice problem to a quantum impurity embedded in a self-consistently determined conduction electron bath. As a canonical model for strong correlation physics, it has been extended in various directions, including the periodic Anderson model for heavy fermion physics [4–9] and the Anderson-Holstein model for studying the interplay between electron-electron and electron-phonon interactions [10–21].

For an impurity with Q d-electrons (where Q is less than the total number of d-electron flavors N), the SIAM describes the low energy formation of a free local moment that becomes spin-screened by the conduction sea, creating a spin singlet bound state- known as the Kondo effect. This bound state formation represents the strong coupling fixed point of the Kondo and the infinite U Anderson models, where valence fluctuations  $Q \rightleftharpoons Q \pm 1$ , corresponding to lower and upper Hubbard bands, have been integrated out of the theory. However, depending on the degree of mixed valence, these valence fluctuations may influence the low energy physics.

The ideas from the SIAM has also recently been applied to two dimensional van der Waals materials such as magic-angle twisted bilayer graphene where the Bistritzer-MacDonald model was mapped to a topological heavy fermion model [22–24] and the key energy scales are set by the impurity limit, allowing methods and

ideas from the heavy fermion community to be applied to MATBG [25–31]. Another example is gate-tunable AB-stacked MoTe<sub>2</sub>/WSe<sub>2</sub> moiré bilayers [32] which exhibits physics spanning from Kondo to mixed valence regimes [33]. Capturing this broad spectrum of low energy behavior presents a challenge for theoretical frameworks ("impurity solvers"). When the Q is a fixed integer, the upper and lower Hubbard bands corresponding to the impurity valence fluctuations  $Q \rightleftharpoons Q \pm 1$  can be integrated out of the theory giving rise to the Kondo model. The Kondo limit can be exactly solved using Bethe ansatz [34] and treated approximately using meanfield theory. Mean-field theory captures describes the Kondo resonance physics of the strong-coupling limit, describing an Abrikosov-Suhl resonance with a width of order the Kondo temperature  $T_K$ , corresponding to the inverse lifetime of the bound state. To go beyond the static mean-field theory to describe both the Kondo and mixed valence dynamics, several approaches have been developed which generalize the slave boson approach. Here we recapitulate the two most prominent: slave bosons and slave rotors.

The original slave boson representation [35–37] describes the projected Hubbard operators [38],  $X_{\sigma 0} \equiv f_{\sigma}^{\dagger} P_0$  relevant to infinite-U Anderson or Hubbard models as

$$d^{\dagger}_{\sigma}P_0 \to f^{\dagger}_{\sigma}b,$$
 (1)

where  $P_0 = |d^0\rangle\langle d^0|$ , which projects into the empty state, is replaced by a boson b. This factorization into canonical fields converts the non-holonomic constraint  $n_d \leq 1$  of the infinite U Hubbard model into a holonomic constraint accessible to field-theory such that

$$Q = n_b + n_f, \qquad [H, Q] = 0 \tag{2}$$

where  $n_b = b^{\dagger}b$  and  $n_f = \sum_{\sigma} f_{\sigma}^{\dagger} f_{\sigma}$  are the number of bosons and spinons respectively. Since Q commutes with the Hamiltonian, it generates a gauge symmetry that polices the constraints. By choosing Q = 1, we recover the infinite U models. In SU(N) models, in which the spin component  $\sigma \in \{1, 2...N\}$  can have N possible values, Q can have any integer value between 1 and N-1. Increasing N, keeping Q/N = q fixed generates a family of

<sup>\*</sup> liam.lh.lau@physics.rutgers.edu

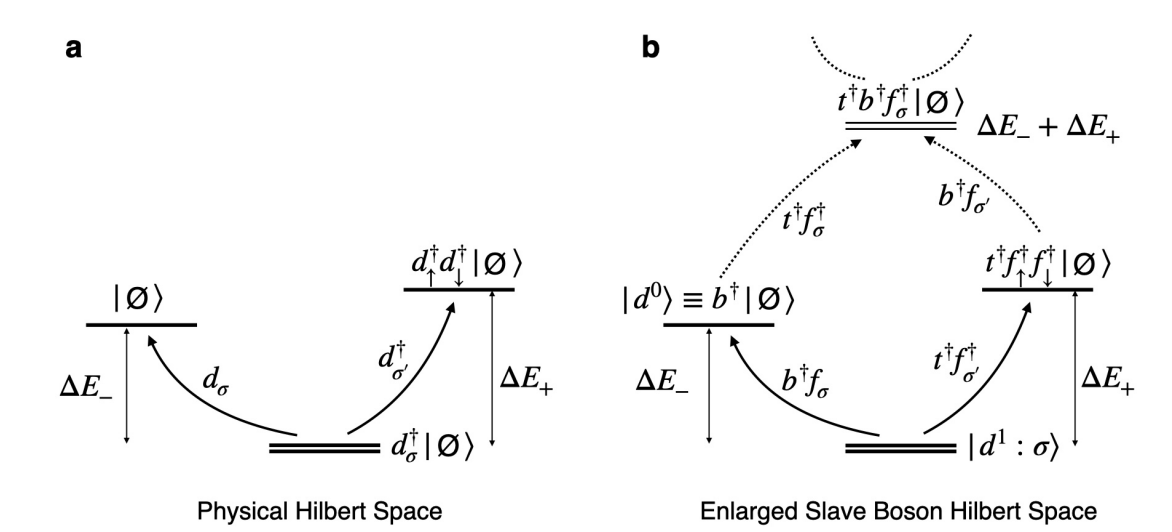


FIG. 1. Schematic of the atomic energy levels of the single impurity Anderson model shown in (a) the physical d-electron Hilbert space and (b) the enlarged slave boson Hilbert space. In the physical Hilbert space,  $\Delta E_{-}$  and  $\Delta E_{+}$  represent the excitation energies to remove or add a d-electron to the singly occupied state  $d_{\sigma}^{\dagger}|\varnothing\rangle$ , respectively. The slave boson representation accurately captures the physical atomic energy levels when the excitation energies  $\Delta E_{\pm}$  are sufficiently large to suppress transitions to fictitious states (dashed lines).

models that with a controlled large N expansion. The slave boson method preserves the commutation algebra of Hubbard operators, while enabling analytic calculations of the fluctuations around mean-field theory. However its great draw-back is that it treats valence fluctuations asymmetrically, only describing charge fluctuations to the lower valence state  $d^1 \rightleftharpoons d^0$  relevant to infinite U models.

Subsequent work [39] generalized the slave boson method to include double occupation by introducing four bosons,

$$d_{\sigma} = f_{\sigma} \tilde{z}_{\sigma}; \quad \tilde{z}_{\sigma} = e^{\dagger} p_{\sigma} + p_{-\sigma}^{\dagger} g, \tag{3}$$

where the first and second terms corresponds to the transitions  $d^1 \to d^0$  and  $d^2 \to d^1$  respectively. This representation requires two constraints

$$Q = e^{\dagger}e + \sum_{\sigma} p_{\sigma}^{\dagger} p_{\sigma} + g^{\dagger}g = 1$$
  
$$f_{\sigma}^{\dagger} f_{\sigma} = p_{\sigma}^{\dagger} p_{\sigma} + g^{\dagger}g. \tag{4}$$

Although able to reproduce the Gutzwiller projection, analytic treatments of the fluctuations are cumbersome.

By contrast, slave rotors [40, 41], employ the phase  $\theta$ , dual to the impurity charge as the collective variable,

$$d_{\sigma}^{\dagger} \to f_{\sigma}^{\dagger} e^{i\theta},$$
 (5)

with the constraint,

$$\frac{N}{2} = n_f - L_z,\tag{6}$$

where the rotor operators are expressed in terms of angular momentum operators, identifying  $L_z = -id/d\theta$ , and

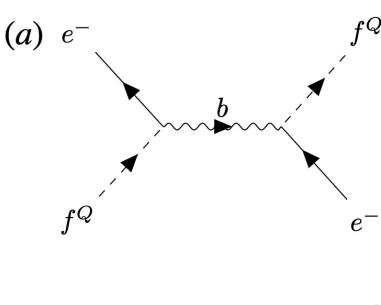
 $L_{\pm}=e^{\pm i\theta}$ . This decoupling (5) can be regarded as a unitary transformation  $d_{\sigma}^{\dagger}=e^{-i\theta n_f}f_{\sigma}^{\dagger}e^{i\theta n_f}$ , and as such, it preserves the canonical commutation relations. This description has the advantage that it treats valence fluctuations symmetrically, but the calculation of fluctuations is more involved than in the slave boson theory.

The basic O(2) slave rotor theory, with a single rotor field, does not admit a controlled large-N mean-field expansion, so fluctuations around the saddle-point solution remain strong. To address this, Florens and Georges [40] introduced an O(2M) generalization with M rotor field components, extending the charge symmetry and enabling a controlled large-M limit. This approach reproduces the atomic limit at half-filling when the interaction is properly normalized to preserve the excitation gap of U, but it also introduces complications since the O(2M) rotor spectrum contains degeneracies and charge dependencies not present in the original O(2) case, making the mapping less accurate away from half-filling.

The aim of this paper is to build on the boson and rotor approaches, introducing a bosonic representation that combines an economy of calculation with a symmetric treatment of valence fluctuations. The key representation

$$d_{\sigma}^{\dagger} \to f_{\sigma}^{\dagger} \left( b + t^{\dagger} \right),$$
 (7)

involves a spinon  $f_{\sigma}^{\dagger}$  and two bosonic partons, "top" (t) and "bottom" (b), that that keep track of addition and removal of charge, respectively. This representation preserves the conserved charge  $Q = n_f + b^{\dagger}b - t^{\dagger}t$  which is set to an integer value in the physical subspace [37]. We note that this representation of the atomic problem expands the Hilbert space (see Fig. 1) and is therefore not entirely faithful. However, when the atomic excitations  $\Delta E_{\pm}$  are



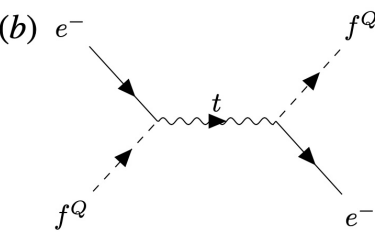


FIG. 2. Feynman diagrams illustrating how (a) the exchange of a b boson keeps mediates fluctuations  $d^Q \rightleftharpoons d^{Q-1} + e^-$ . (b) Exchange f a t boson mediates fluctuations  $d^Q + e^- \rightleftharpoons d^{Q+1}$ .

sufficiently large, fictitious states associated with multiple top or bottom bosons are suppressed, and the Feynman diagrams for single top or bottom boson exchange accurately track the valence fluctuations (Fig. 2).

The connection between our two slave boson representation and the slave rotor representation emerges through their shared constraint structures and underlying commutation algebra. If we generalize the rotor constraint (6) to be for arbitrary Q rather than for half-filling Q = N/2, the generalized rotor constraint  $Q = n_f - L_z$  directly parallels the two boson constraint  $Q = n_f - \left(-b^\dagger b + t^\dagger t\right)$ , suggesting a correspondence between  $L_z$  and  $\left(t^\dagger t - b^\dagger b\right)$ . More fundamentally, the commutation relations of the U(1) angular momentum operators,  $[L_z, L_\pm] = \pm L_\pm$  and  $[L_+, L_-] = 0$ , are reproduced by the in the two slave boson representation  $([t^\dagger t - b^\dagger b, b + t^\dagger] = b + t^\dagger, [t^\dagger t - b^\dagger b, b^\dagger + t] = -(b^\dagger + t)$ , and  $[b + t^\dagger, b^\dagger + t] = 0$ , establishing that both formulations represent the same algebraic structure.

We show that the antisymmetric combination  $b-t^{\dagger}$  decouples from the theory, leading to an effective theory for the symmetric combination  $s=b+t^{\dagger}$ , allowing a reduction of the theory to a single symmetric s-boson theory. At the end of this procedure, the original slave boson approach can be transformed into the s-parton formulation by replacing  $b \to s$  in the hybridization and

$$b^{\dagger}(\partial_{\tau} + \lambda)b \to \frac{1}{U} s^{\dagger} \left[ \left(\frac{U}{2}\right)^2 - (\partial_{\tau} + \lambda)^2 \right] s.$$
 (8)

This term replaces the single pole at  $\omega = \lambda$  by a double pole at  $\omega = \lambda \pm U/2$  in the s-boson. With this economic transformation the slave boson approach can be upgraded to include symmetric valence fluctuations without having to recalculate the fermionic RPA bubbles. We further show that the infinite U and Kondo limits can be recovered from our approach. Contrary to the O(2) rotor

theory, our s-boson theory has a controlled large-N expansion due to  $\bar{s}s = |s|^2 \sim \mathcal{O}(N)$  in the condensed phase.

This article is organized as follows. In section II we introduce a representation of the impurity fermionic operators in terms of a spinon, top t and bottom b boson, to keep track of positive and negative valence fluctuations. We show that in the finite U multiorbital SIAM, the representation can be reduced to a single s-boson which symmetrically captures the lower and upper Hubbard band physics. In section III, we present the result of our single s-boson approach to the SIAM, showcasing calculating the local spectral function and charge susceptibility. In the discussion section IV, we build on the algebraic relationship between our s-boson formulation and slave rotor approach, demonstrating the equivalence of their actions for the SIAM under a unified functional integral approach when we forgo the s-boson's large-Nexpansion by normalizing the s-boson algebra. We end with a short discussion on the treatment of strong mixed valence where fluctuations into the fictitious states with multiple t and b bosons (Fig. 1) are not energetically suppressed and suggest future extensions of our method.

#### II. METHOD

#### A. Atomic and Single Impurity Anderson Model

We first recapitulate the physics of the SIAM, starting with the atomic limit for an N-fold degenerate atomic level with a SU(N) symmetric onsite Coulomb interaction,

$$H_A = \epsilon_d n_d + \frac{U}{2} (n_d - N/2)^2$$
. (9)

Here,  $\epsilon_d$  is d-level position at half filling, and the Coulomb interaction is defined relative to half-filling,  $n_d = \sum_{\sigma} d_{\sigma}^{\dagger} d_{\sigma}$ , where  $\sigma = 1, 2, ... N$  labels the spin and orbital degrees of freedom.

In the SIAM, electrons can tunnel into and out of of the atomic level (9) to a conduction sea with dispersion  $\epsilon_{\mathbf{k}}$ .

$$H_c = \sum_{\mathbf{k}\sigma} \epsilon_{\mathbf{k}} c_{\mathbf{k}\sigma}^{\dagger} c_{\mathbf{k}\sigma}, \tag{10}$$

through the hybridization

$$H_{\rm hyb} = \frac{V_0}{\sqrt{N}} \sum_{\mathbf{k}\sigma} \left( c_{\mathbf{k}\sigma}^{\dagger} d_{\sigma} + \text{h.c.} \right). \tag{11}$$

In general, the hybridization can be momentum dependent, but in this work we will take the simplified scenario where the hybridization is momentum independent and the conduction bath is featureless and has a constant density of states  $\rho$ . The full SIAM Hamiltonian is,

$$H = H_{\rm c} + H_A + H_{\rm hvb}. \tag{12}$$

The hybrdization between the atom and a conduction bath allows for the valence of the atom to fluctuate ( $Q \rightleftharpoons Q \pm 1$ ) around each integer Q with ionization energies,

$$\Delta E_{+}^{Q} = E_{Q+1} - E_{Q} = \tilde{\epsilon}_{d} + U/2,$$

$$\Delta E_{-}^{Q} = E_{Q-1} - E_{Q} = -\tilde{\epsilon}_{d} + U/2.$$
(13)

where we have introduced the notation

$$\tilde{\epsilon}_d = \epsilon_d + U(Q - N/2) \tag{14}$$

for the d-level position at doping away from half filling. The atomic ground-state has  $n_d = Q$ , provided  $|\tilde{\epsilon}_d| > U/2$ , i.e provided  $\epsilon_d$  lies within U/2 of U(Q - N/2). The upper and lower Hubbard band positions correspond create resonances in the d-electron spectral function at energies

$$\omega_{+} = \Delta E_{+}^{Q}, \quad \omega_{-} = -\Delta E_{-}^{Q}, \tag{15}$$

which are separated by the onsite Coulomb scale U.

## B. Slave Boson Representation of SIAM

Unlike the infinite U Anderson model, we now need to keep track of charge fluctuations due to adding and re-moving an electron from the atom. We do so by first rewriting the physical d-electron as the product of a spinon  $f_{\sigma}$  which lives in a constrained Hilbert space and introduce two bosons, t and b, the "top" and "bottom" bosons which keep track of the charge fluctuations into the Q+1 and Q-1 valence states, respectively. We then write

$$d_{\sigma}^{\dagger} \rightarrow f_{\sigma}^{\dagger}(b+t^{\dagger}).$$
 (16)

The inclusion of these slave bosons expand the Hilbert space, therefore a softened constraint is required to fix it back to be the physical Hilbert space,

$$n_f + n_b - n_t = Q. \tag{17}$$

Q describes a fixed gauge charge of the mixed valent system, in which the top and bottom bosons have opposite gauge charge. Within the physical subspace constrained by Eq. 17, the Hamiltonian,

$$\tilde{H} = H_c + \frac{V_0}{\sqrt{N}} \sum_{\mathbf{k}\sigma} \left( c_{\mathbf{k}\sigma}^{\dagger} f_{\sigma} \left( b^{\dagger} + t \right) + \text{h.c.} \right)$$

$$+ \Delta E_{-}^{Q} b^{\dagger} b + \Delta E_{-}^{Q} t^{\dagger} t.$$
(18)

provides a low-energy description of the single-impurity Anderson model. As an important initial check, we note that if the conduction bath is particle-hole symmetric, i.e  $\epsilon_{\mathbf{k}} = -\epsilon_{-\mathbf{k}}$ , then under the particle-hole transformation

$$c_k \rightarrow c_{-k}^{\dagger}, \qquad f \rightarrow f^{\dagger}, \qquad t \rightarrow b^{\dagger}$$
  
 $\lambda \rightarrow -\lambda, \qquad Q \rightarrow N - Q, \qquad \epsilon_d \rightarrow -\epsilon_d \qquad (19)$ 

the action  $H + \lambda(n_f + n_b - n_t - Q)$  is invariant.

The partition function in the Gibb's ensemble of definite Q is then written

$$Z_Q = \int_{\lambda_0}^{\lambda_0 + 2\pi i k_B T} \frac{d\lambda}{2\pi i k_B T} \text{Tr} \left[ e^{-\beta \left( H + \lambda (n_f + n_b - n_t - Q) \right)} \right]$$
(20)

where the chemical potential  $\lambda$ , integrated along the imaginary axis from  $\lambda = \lambda_0$  to  $\lambda = \lambda_0 + 2\pi i k_B T$  imposes the constraint on the gauge charge(17). By extending the  $\lambda$  integral along the imaginary axis, we can then rewrite the partition function as a path integral,

$$Z_Q = \int D[B, F] \exp\left[-\int_0^\beta d\tau L\right],$$
  

$$L = L_F + L_{\text{hvb}} + L_B, \tag{21}$$

where  $D[B] \equiv D[\bar{b}, b, \bar{t}, t, \lambda]$  describes the measure of integration over the slave bosons b, t and the constraint field  $\lambda$ , while  $D[F] = D[c^{\dagger}, c, f^{\dagger}, f]$  denote the measures of integration over the conduction and f-electrons.

$$L_F = \sum_{\mathbf{k},\sigma} c_{\mathbf{k}\sigma}^{\dagger} (\partial_{\tau} + \epsilon_{\mathbf{k}}) c_{\mathbf{k}\sigma} + \sum_{\sigma} f_{\sigma}^{\dagger} (\partial_{\tau} + \lambda) f_{\sigma}$$
 (22)

is the Lagrangian for the fermions.

$$L_{\text{hyb}} = \frac{V_0}{\sqrt{N}} \sum_{\mathbf{k}\sigma} \left( c_{\mathbf{k}\sigma}^{\dagger} f_{\sigma} \left( \bar{b} + t \right) + \text{H.c.} \right), \tag{23}$$

describes the hybridization and

$$L_B = \bar{b}(\partial_{\tau} + \Delta E_{-}^{Q} + \lambda)b + \bar{t}(\partial_{\tau} + \Delta E_{+}^{Q} - \lambda)t - \lambda Q$$
(24)

is the Lagrangian for the bosons. The constraint field  $\lambda$  couples to the f-electron in (22), and to the bottom and top bosons b and t in (24) with opposite charge.

# C. Effective Action

By combining the bottom with the conjugated top boson in symmetric and antisymmetric combinations

$$s = (b + \bar{t}), \quad a = (b - \bar{t}),$$
 (25)

we can rewrite the hybridization and atomic Lagrangians (23) and (24) as,

$$L_{\text{hyb}} = \frac{V_0}{\sqrt{N}} \sum_{\mathbf{k}\sigma} \left( c_{\mathbf{k}\sigma}^{\dagger} f_{\sigma} s + \text{H.c.} \right),$$

$$L_B = \left[ \frac{1}{4} (\bar{s} + \bar{a}) (\partial_{\tau} + \frac{U}{2} - \tilde{\epsilon}_d + \lambda) (s + a) + \frac{1}{4} (s - a) (\partial_{\tau} + \frac{U}{2} + \tilde{\epsilon}_d - \lambda) (\bar{s} - \bar{a}) - \lambda Q \right],$$
(26)

The antisymmetric boson a decouples from the fermions, and we can integrate it out (see Appendix A for details), so that the bosonic action

$$L_B = \frac{1}{U}\bar{s}\left(\frac{U^2}{4} - (\partial_\tau + \lambda - \tilde{\epsilon}_d)^2\right)s - \lambda Q. \tag{27}$$

now contains two poles at  $\omega = \lambda - \tilde{\epsilon}_d \pm U/2$ , corresponding to the upper and lower Mott bands. The complete action for our s-boson reformulation is then

$$S = \int_{0}^{\beta} d\tau \left[ \frac{1}{U} \bar{s} \left( \frac{U^{2}}{4} - (\partial_{\tau} + \lambda - \tilde{\epsilon}_{d})^{2} \right) s + \sum_{\mathbf{k}, \sigma} c_{\mathbf{k}\sigma}^{\dagger} (\partial_{\tau} + \epsilon_{\mathbf{k}}) c_{\mathbf{k}\sigma} + \sum_{\sigma} f_{\sigma}^{\dagger} (\partial_{\tau} + \lambda) f_{\sigma} + \frac{V_{0}}{\sqrt{N}} \sum_{\mathbf{k}\sigma} \left( c_{\mathbf{k}\sigma}^{\dagger} f_{\sigma} s + \text{H.c.} \right) - \lambda Q \right].$$
(28)

The economy of our approach is thus revealed, for apart from the modified bosonic action, i.e the modified atomic physics incorporating the upper and lower Mott bands, this is identical to the original slave boson formulation. This action has a controlled large-N expansion due to  $|s| \sim \mathcal{O}(\sqrt{N})$ , thus every term in (28) scales with N.

## D. Recovery of the infinite U and Kondo limits

Let us now verify that this action recovers the well known infinite U and Kondo limits of the Anderson model. We first factorize

$$L_{B} = \frac{1}{U}\bar{s}\left[\left(\frac{U}{2} + (\partial_{\tau} + \lambda - \tilde{\epsilon}_{d})\right)\left(\frac{U}{2} - (\partial_{\tau} + \lambda - \tilde{\epsilon}_{d})\right)\right]s - \lambda Q$$

$$= \frac{1}{U}\bar{s}\left[\left(\partial_{\tau} + \lambda - E_{d}\right)\left(U + E_{d} - \partial_{\tau} - \lambda\right)\right]s - \lambda Q,$$
(29)

where we have redefined  $E_d = \tilde{\epsilon}_d - U/2$ . The infinite U limit is obtained by taking  $U \to \infty$ , maintaining  $E_d$  fixed, allowing the second term of (29) to be replaced by U, recovering the action of the infinite U Anderson model,

$$L_B^{U=\infty} = \bar{s} \left( \partial_\tau + \lambda - E_d \right) s - \lambda Q. \tag{30}$$

The Kondo limit occurs when the positions of the upper and lower Mott bands exceed the band-width. In this situation, the high-frequency charge dynamics of the s-boson are eliminated, and since the d-level position is far smaller than the Mott band energies, we can set the frequency  $\partial_{\tau} + \lambda \to 0$  in  $L_B$ . Rescaling s as a hybridization field by writing  $\frac{V_0}{\sqrt{N}}s = V$ , the resulting Kondo action is,

$$S_{K} = \int_{0}^{\beta} d\tau \left[ \sum_{\mathbf{k},\sigma} c_{\mathbf{k}\sigma}^{\dagger} (\partial_{\tau} + \epsilon_{\mathbf{k}}) c_{\mathbf{k}\sigma} + \sum_{\sigma} f_{\sigma}^{\dagger} (\partial_{\tau} + \lambda) f_{\sigma} + \sum_{\mathbf{k}\sigma} (\bar{V} c_{\mathbf{k}\sigma}^{\dagger} f_{\sigma} + \text{H.c.}) + N \frac{\bar{V}V}{J} - \lambda Q \right], \tag{31}$$

This recovers the well-known Newns-Read formulation of the Coqblin-Schrieffer model, but now, with the well-known Schrieffer-Wolff expression for the Kondo coupling constant,

$$J = \frac{V_0^2}{U/2 - \tilde{\epsilon}_d} + \frac{V_0^2}{U/2 + \tilde{\epsilon}_d}$$
 (32)

## E. Mean-field Theory

By integrating (27) over the fermionic fields, we obtain the effective action in terms of  $\lambda$  and s,

$$Z = \int D[\lambda, s] \exp(-S_E[\lambda, s]). \tag{33}$$

Seeking a static mean-field theory, varying  $S_E$  with respect to s we obtain

$$\frac{1}{U} \left( \frac{U^2}{4} - (\lambda - \tilde{\epsilon}_d)^2 \right) s + \frac{V_0}{\sqrt{N}} \sum_{\mathbf{k}\sigma} \langle c_{\mathbf{k}\sigma}^{\dagger} f_{\sigma} \rangle_s = 0, \quad (34)$$

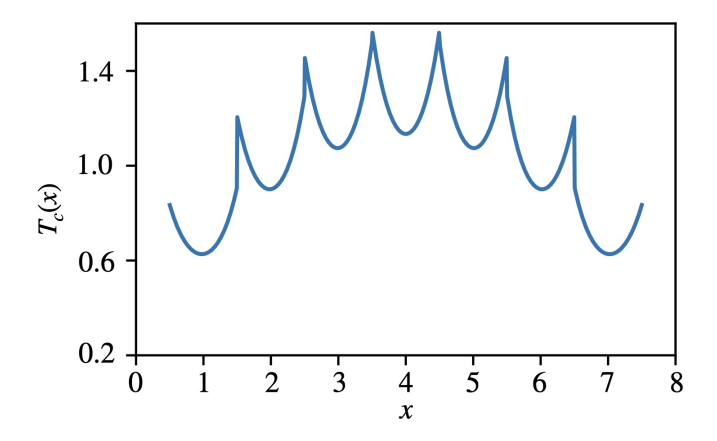


FIG. 3. Mean-field transition temperature  $T_c$  into the Kondo phase versus electron filling x for N=8,  $\Delta=7.5$ ,  $T_K/\Delta=0.13$ ,  $U/\Delta=13.3$ . The d-level position from half filling  $\tilde{\epsilon}_d$  is taken to vary linearly from -U/2 to U/2 between half-integer fillings, with stepwise jumps in the impurity filling factor q=Q/N as Q is increased to Q+1 in the calculation.  $T_c$  is maximized at half-integer fillings where impurity mixed valence between charge states Q and  $Q\pm 1$  is greatest.

while varying  $S_E$  with respect to  $\lambda$ , the mean-field constraint (17) now becomes,

$$\langle n_f \rangle + 2 \frac{(\tilde{\epsilon}_d - \lambda)}{U} |s|^2 = Q.$$
 (35)

The second term in this expression is identified as the expectation value of  $|b|^2 - |t|^2$ , denoting the deviation from integral valence. We now present some analytical results for a single impurity Anderson model with a conduction sea with a constant density of states  $\rho$ . If we assume a constant density of conduction states  $\rho$  with a bandwidth 2D, then the mean-field impurity free energy is given by (see Appendix B for details),

$$F = -TN \sum_{\omega_n < D_c} \ln\left[\lambda + i\tilde{\Delta}_n - i\omega_n\right] + \frac{|s|^2 V_0^2}{J(\lambda)} - \lambda Q. \quad (36)$$

Here  $D_c = \min(D, U/2)$ , the high-energy cutoff, depends on the relative size of the bandwidth D and the Coulomb interaction U, while  $i\tilde{\Delta}_n = i\pi\rho V_0^2|\tilde{s}|^2\mathrm{sgn}(n)$  is the largecutoff approximation for the f-electron self energy, where  $\tilde{s} = s/\sqrt{N}$ . Lastly, the  $\lambda$ -dependent Kondo coupling has the Schrieffer-Wolff form,

$$J(\lambda) = \frac{V_0^2}{U/2 + \lambda - \tilde{\epsilon}_d} + \frac{V_0^2}{U/2 - \lambda + \tilde{\epsilon}_d}$$
(37)

Within mean-field theory, the Kondo effect has two effects, firstly to float the f-level  $\lambda$  at the Fermi level, and secondly to renormalize the resonant level hybridization width from the bare hybridization width  $\Delta = \pi \rho V_0^2$  to  $\tilde{\Delta} = \pi \rho V_0^2 |\tilde{s}|^2$ .

Using the complex d-level position

$$\xi = \lambda + i\tilde{\Delta},\tag{38}$$

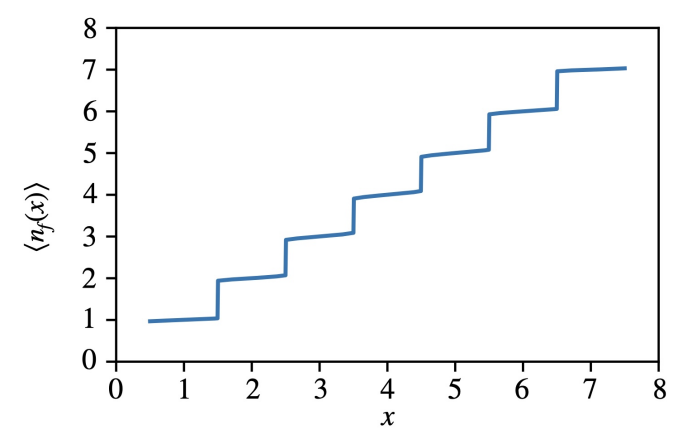


FIG. 4. Mean-field impurity valence at zero temperature as a function of electron filling x for N=8,  $\Delta=7.5$ ,  $T_K/\Delta=0.13$ ,  $U/\Delta=13.3$ . The d-level position from half filling  $\tilde{\epsilon}_d$  is taken to vary linearly from -U/2 to U/2 between half-integer fillings, with stepwise jumps in the impurity filling factor q=Q/N as Q is increased to Q+1 in the calculation.

whose real and imaginary parts respectively represent the position and width of the resonant level, the mean-field Free energy can be written as

$$F = N \operatorname{Im} \left[ 2iT \ln \tilde{\Gamma}(\xi) - \frac{\xi}{\pi} \ln \frac{D_c}{2\pi iT} \right] + \frac{|s|^2 V_0^2}{J(\lambda)} - \lambda Q \quad (39)$$

where  $\tilde{\Gamma}(\xi) = \Gamma\left(\frac{1}{2} + \frac{\xi\beta}{2\pi i}\right)$ , is a short-hand for the gamma function and  $\beta$ , the inverse temperature. We can also rewrite the free energy in the compact form  $F = N \text{Im} F_c$ , where

$$F_c = 2iT \ln \tilde{\Gamma}(\xi) - \frac{\xi}{\pi} \ln \frac{T_K(\lambda)e^{i\pi q}}{2\pi iT},\tag{40}$$

where  $T_K(\lambda) = D_c \exp\left[-\frac{1}{\rho J(\lambda)}\right]$  is the  $\lambda$ -dependent Kondo temperature and  $q = \frac{Q}{N}$ . In the Kondo limit, we can neglect the  $\lambda$  dependence of the Kondo coupling constant, setting  $J = J(\lambda = 0)$ . In this limit, we obtain the saddle point equations by differentiating (40) with respect to  $\xi$ . Setting  $\partial F_c/\delta \xi = 0$ , we obtain

$$\tilde{\psi}(\xi) = \ln\left(\frac{T_K e^{i\pi q}}{2\pi i T}\right),$$
 (41)

where we denote,  $\tilde{\psi}(\xi) = \psi\left(\frac{1}{2} + \frac{\xi\beta}{2\pi i}\right)$ , and  $\psi(z) = d\ln\Gamma(z)/dz$  is the digamma function.  $T_K = T_K(\lambda)|_{\lambda=0} = D_c \exp\left[-\frac{1}{\rho J}\right]$  is the Kondo temperature. At low temperature, we can approximate  $\tilde{\psi}(z) = \ln\left(\frac{z}{2\pi i T}\right)$ , so we obtain simply  $\xi = \lambda + i\tilde{\Delta} = T_K e^{i\pi q}$ , recovering the large N limit of the SU(N) Kondo model, but with the finite U Schrieffer-Wolff form of the coupling constant J(32).

In the strongly mixed valent regime, we must take account of the  $\lambda$  dependence of the Kondo coupling constant. In this case, the mean field equation from varying

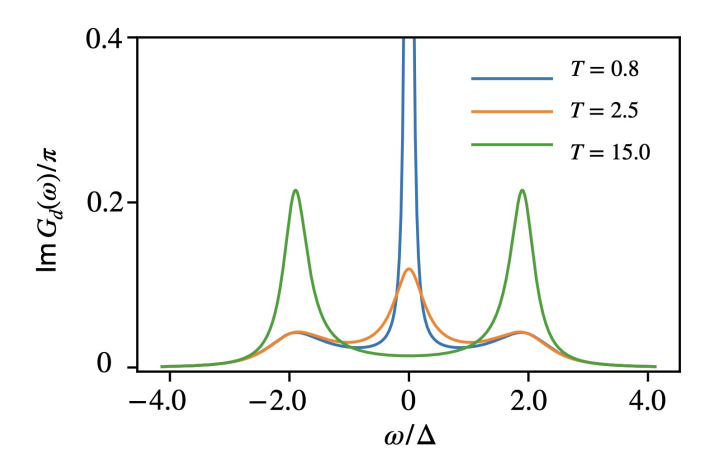


FIG. 5. The full physical d-electron spectral function for the symmetric limit,  $\Delta = 7.5$ ,  $\tilde{\epsilon}_d = 0.0$ ,  $U/\Delta = 4.0$  for different temperatures as labeled in the figure.

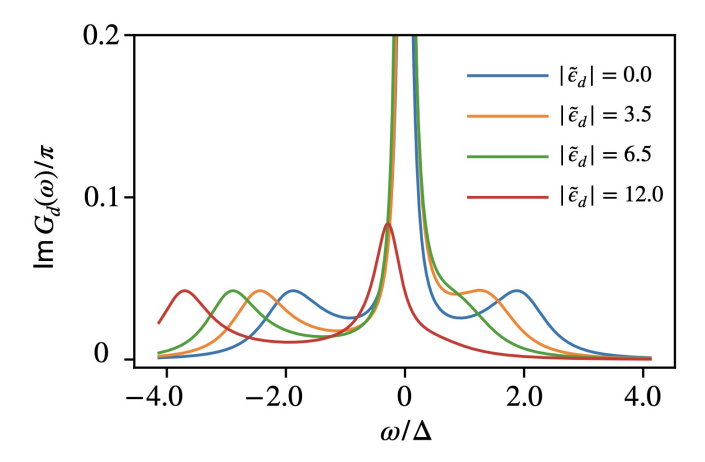


FIG. 6. The *d*-electron spectral function for the asymmetric limit,  $\Delta$  = 7.5, T = 1.5, and  $U/\Delta$  = 4.0 for different *d*-electron levels  $\epsilon_d$  =  $-|\epsilon_d|$ .

(39) with respect to  $\tilde{s}$  can be written as,

$$\operatorname{Re}\left[\tilde{\psi}(\xi) - \ln\left(\frac{\beta T_K(\lambda)}{2\pi}\right)\right] = 0. \tag{42}$$

The saddle-point condition  $\partial F/\partial \lambda = 0$  is

$$\frac{1}{\pi} \operatorname{Im} \left[ \tilde{\psi}(\xi) + \frac{i\pi}{2} \right] + 2 \frac{(\tilde{\epsilon}_d - \lambda)}{U} |\tilde{s}|^2 = q, \tag{43}$$

where the second term is recognized as the deviation from integral valence found in (35). We can combine the two equations in complex form,

$$\tilde{\psi}(\xi) - \ln\left(\frac{T_K(\lambda)e^{i\pi q}}{2\pi i T}\right) = -2\pi i \frac{\tilde{\epsilon}_d - \lambda}{U} |\tilde{s}|^2. \tag{44}$$

The transition temperature  $T_c$  into the mean-field Kondo phase as a function of electron filling x can be found by solving (44) in the limit where  $\tilde{s} = 0$ , and  $f(\lambda) = q$ ,

where  $f(\lambda) = 1/(e^{\beta\lambda} + 1)$  is the Fermi function. Figure 3 shows  $T_c$  versus filling x for N=8, where the impurity filling factor q=Q/N is taken to increase stepwise at half-integer filling x as the number d-electrons in the impurity jumps from Q to Q+1. The d-level from half-filling  $\tilde{\epsilon}_d$  is taken to vary linearly from -U/2 to U/2 between these jumps. The resulting  $T_c(x)$  exhibits a "Millennium dome" structure with maxima at half-integer fillings (where mixed valence is greatest) and minima at integer fillings (where the Kondo limit holds), with interpolation between each cusp as q jumps. Overall, we find  $T_c$ , characterizing the cross-over to the Fermi liquid, is maximized at half-integer fillings, and is largest near half filling Q = N/2.

At zero temperature, (44) can be written as,

$$\ln\left(\frac{\xi}{T_{K}e^{i\pi q}}\right) = \frac{\pi}{N\Delta_{0}U}\left[\left(\xi - \tilde{\epsilon}_{d}\right)^{2} + \operatorname{Im}\left[\xi\right]^{2}\right], \quad (45)$$

which can be solved for the zero temperature value of the complex d-level  $\xi$ . We can then immediately calculate the zero temperature mean-field impurity valence  $\langle n_f \rangle$ ,

$$\langle n_f \rangle = Q - 2 \frac{(\tilde{\epsilon}_d - \lambda)}{U} |s|^2 = \frac{N}{\pi} \operatorname{Im} \ln [\xi].$$
 (46)

Figure 4 shows the impurity valence  $\langle n_f \rangle$  as a function of electron filling x for N=8, where the impurity filling factor q=Q/N is again taken to increase stepwise at half-integer filling x as the number d-electrons in the impurity jumps from Q to Q+1. The d-level from half-filling  $\tilde{\epsilon}_d$  is also taken to vary linearly from -U/2 to U/2 between these jumps.

Similar to the slave rotor approach [40, 41], which exhibits reduced accuracy away from half filling (Q = N/2), our theoretical framework becomes unreliable when the system deviates significantly from integer occupancy values Q. To mitigate this limitation, we have employed a stitching procedure where Q is manually increased stepwise with  $\tilde{\epsilon}_d$  resetting, as discussed previously for Figs. 3 and 4. This approach enables accurate calculation of physical quantities such as impurity occupancy as a function of filling x across the entire parameter range as shown in Fig. 4. However, there is no clear prescription of how to increase Q and  $\tilde{\epsilon}_d$  systematically.

# F. Gaussian Fluctuations

The dynamic valence fluctuations of the SIAM can be economically captured within the method by including fluctuations around the mean-field solution

$$s(\tau) = s + \sqrt{N}\delta s(\tau) \tag{47}$$

to second order. By expanding  $S_E$  to Gaussian order, we obtain

$$\Delta S_{E} = N \sum_{i\nu_{m}} \bar{s}_{m} s_{m} \left\{ \frac{1}{U} \left[ \left( \frac{U}{2} \right)^{2} - \left( \lambda - \tilde{\epsilon}_{d} - i\nu_{m} \right)^{2} \right] - \chi_{0} (i\nu_{m}) \right\} - \frac{N}{2} \sum_{i\nu_{m}} \left[ \bar{s}_{m} \bar{s}_{-m} + s_{m} s_{-m} \right] \chi_{A} (i\nu_{m})$$
(48)

where the fluctuations of s is written in Matusbara frequency  $s_m \equiv \int_0^\beta e^{i\nu_m\tau} \delta s(\tau)$ , and the hybridization susceptibilities  $\chi_0(i\nu_m)$  and  $\chi_A(i\nu_m)$  are unchanged from the infinite U slave boson case [37].

Let us consider the "normal state", where  $\tilde{s} = 0$  and the anomalous Bose self-energy  $\Pi_A$  vanishes. The first term in the curly bracket of (48) derives from the kinematics of the s-boson in the effective action (27), while the second term is described by the one-loop Kondo susceptibility  $\chi_0(i\nu_m)$  which is,

$$-\chi_0(i\nu_m) = \frac{\Delta}{\pi} \left( \left[ \tilde{\psi}(\xi + i\nu_m) - \tilde{\psi}(\xi) \right] \right)^* + \frac{\Delta}{\pi} \operatorname{Re} \left[ \tilde{\psi}(\xi) - \ln \frac{D}{2\pi i T} \right], \tag{49}$$

(see Appendix C for the full expression from [37]). Here,  $\Delta = \pi \rho V_0^2$  is the bare hybridization width. Recall that the complex d-level position (38)  $\xi = \lambda + i\tilde{\Delta} = \lambda$  in the normal state, since the imaginary part  $\tilde{\Delta} = \Delta |\tilde{s}|^2 = 0$  vanishes. We can immediately write down the inverse propagator for the s-boson Gaussian fluctuations in the normal state,

$$\frac{D_s(i\nu_m)^{-1}}{N} = \chi_0(i\nu_m) - \frac{U}{4} \left[ 1 - \frac{(\lambda - \tilde{\epsilon}_d - i\nu_m)}{(U/2)^2} \right] (50)$$

# III. APPLICATION TO SINGLE IMPURITY ANDERSON MODEL

This section evaluates how accurately the s-boson theory with Gaussian fluctuations in the "normal" state reproduces the physical properties of the SIAM.

#### A. Spectral Function Results

The physical d-electron as the product of the d-spinon and the s-boson,

$$d_{\sigma}^{\dagger}(\tau) = f_{\sigma}^{\dagger}(\tau)s(\tau). \tag{51}$$

We can then approximate the physical *d*-electron Green's function by factorizing,

$$G_d(\tau) = -\langle \mathcal{T} d_{\sigma}(\tau) d_{\sigma}^{\dagger}(0) \rangle \approx -G_f(\tau) D_s(-\tau)$$
 (52)

Using the convolution theorem,

$$G_d(i\omega_n) = -\frac{1}{\beta} \sum_{i\nu_r} G_f(i\omega_n + i\nu_r) D_s(i\nu_r)$$
 (53)

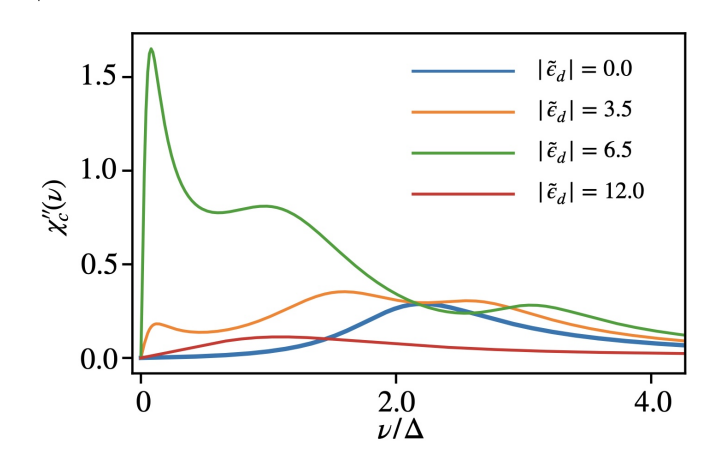


FIG. 7. The dynamical charge susceptibility for  $q=0.5, \Delta=7.5, T=1.5,$  and  $U/\Delta=4.0$  for different d-electron levels.

(See appendix  $\mathbb D$  for more details). The imaginary part of the d-electron propagator is then related to the spectral function,

$$A_{d}(\omega) = G_{d}^{"}(\omega - i\delta)/\pi$$

$$= \frac{1}{\pi} [n_{B}(\lambda - \omega) + q] D_{s}^{"}(\lambda - \omega).$$
 (54)

For the normal state, we take the d-level to be determined by the thermal occupancy of the d-electron  $\lambda = T \ln \left[ (1/q) - 1 \right]$ , where q = Q/N is the ratio of the integer number of d-electrons and the total number of d-electron flavors. In fig. 5, we plot the spectral function of the full physical d-electron in the particle-hole symmetric limit. At high temperatures, there is an upper Hubbard band at  $\omega = U/2$  and lower Hubbard band at  $\omega = -U/2$ . Interestingly, even within the normal phase of the s-boson when it has yet to condense and the anomalous self energy  $\Pi_A(i\nu_m)$  is still zero, a central Kondo resonance begins to develop as the temperature is lowered, reaching it's maximum at the Kondo coherence temperature  $T_c$ .

In fig. 6, we plot the spectral function of the full physical d-electron for the Anderson impurity model as it goes from being symmetric to becoming more and more asymmetric by tuning the  $\tilde{\epsilon}_d$  level. Whilst keeping temperature fixed, the resonance peak does reduce with increasing asymmetry, qualitatively agreeing with the reduction from the Friedel sum rule.

# B. Charge Susceptibility

The dynamic d-electron density can be calculated by noting that it is equal to the dynamic density of the f-spinons. By extremizing the action (27), we obtain the

Gaussian corrections to the constraint (17),

$$\langle n_d(\tau) \rangle = Q + \frac{2}{U} \left\{ \Lambda \bar{s}s + \frac{1}{2} \left( \bar{s} \, \partial_{\tau} [s] - \partial_{\tau} [\bar{s}] s \right) \right\}, \quad (55)$$

where  $\Lambda = \lambda - \tilde{\epsilon}_d$  and we implicitly write  $s \equiv s(\tau)$  as the fluctuation for brevity. From the fluctuations of  $n_d$ , we can calculate the imaginary part of the dynamical charge susceptibility (see Appendix E),

$$\chi_c''(\nu) = \frac{4}{U^2} \int_{-\infty}^{\infty} \frac{d\omega}{\pi} \left( n_B(\omega) - n_B(\omega + \nu) \right) D_s''(\nu + \omega) \times D_s''(\omega) \left[ -\left(\frac{\nu}{2} + \omega\right) + \Lambda \right]^2.$$
 (56)

In Fig. 7, we plot the dynamical charge susceptibility  $\chi_c(\omega)$  for the same parameters as Fig. 6. In the symmetric limit when  $|\epsilon_d| = 0$ , there is a single peak at the atomic excitation energy U/2, corresponding to both the upper and lower Hubbard band positions for the symmetric limit  $|\epsilon_d| = 0$  in Fig. 6, which then splits into two peaks, at the two atomic excitation energies (13), separated by  $2|\epsilon_d|$ . As the upper Hubbard band merges into the central resonance (Fig. 6), the charge susceptibility of the upper Hubbard band increases and a low frequency peak develops, indicating its fermi liquid nature. The low frequency peak disappears upon further lowering of the d-level and the upper Hubbard band becoming the lower Hubbard band for a d valence Q increased by one.

## IV. DISCUSSION

In this paper, we have have introduced a s-boson approach that captures valence fluctuations that both increment and decrement the ionic charge of the finite U single impurity Anderson model. By exactly integrating out the asymmetric bosons dynamics, we have shown that reduces to a *single* symmetric boson ("s-boson") theory in which the upper and lower Hubbard bands are encoded in the boson kinetics. Our calculations of the local spectral function and dynamical charge susceptibility demonstrate that the formation of the Kondo resonance in the SIAM is included in our method, even in the normal state when the s-boson has yet to condense and the anomalous self-energy remains zero. We leave the calculation of the local spectral function and dynamical charge susceptibility in the condensed s-boson state as a future extension of our work.

The s-boson approach provides a efficient upgrade to the original infinite U slave boson method, replacing a single pole excitation at  $\omega = \lambda$  by two excitations of the s-boson at  $\omega = \lambda \pm U/2$ , while preserving the same fermionic RPA bubbles that encode the low energy Kondo resonance information. The s-boson representation correctly recovers both the infinite U and Kondo limits.

We establish the relationship between the slave rotor and s-boson representations through their shared

algebraic structure. Writing the rotor operators in terms of angular momentum operators, identifying  $L_z = -id/d\theta$ , and  $L_{\pm} = e^{\pm i\theta}$ , then the commutation algebra is  $[L_z, L_{\pm}] = \pm L_{\pm}$  and  $[L_+, L_-] = 0$ . Generalizing the rotor constraint (6) from being around half-filling (Q = N/2) to arbitrary integer filling Q,  $n_f = Q - L_z$ , analogous to the s-boson constraint  $n_f = Q - (t^{\dagger}t - b^{\dagger}b)$ . This suggests the identification  $L_z \sim t^{\dagger}t - b^{\dagger}b$ . The s-boson and its two slave boson components satisfy  $[t^{\dagger}t - b^{\dagger}b, s] = s$ ,  $[t^{\dagger}t - b^{\dagger}b, s^{\dagger}] = -s^{\dagger}$  and  $[s, s^{\dagger}] = 0$ , confirming  $(t^{\dagger}t - b^{\dagger}b, s) \sim (L_z, L_+)$  share identical algebras. Thus, the s-boson provides a faithful representation of the U(1) rotation group with  $s \propto L_+$ .

The key distinction between representations lies in the normalization of the algebras, which is inherently linked to whether a controlled large-N saddle-point approximation is present. In our s-boson representation of the SIAM, there is a controlled large-N saddle-point approximation in the condensed phase because  $\bar{s}s = |s|^2 \sim \mathcal{O}(N)$ , whereas the most basic  $\mathcal{O}(2)$  rotor does not because the modulus of the rotor bosonic field is always of order unity. This difference manifests in a generalized anticommutation relation for the s-boson representation of the physical d-electron(7),

$$\{d_{\sigma}, d_{\sigma'}^{\dagger}\} = \{f_{\sigma}s^{\dagger}, f_{\sigma'}^{\dagger}s\} = s^{\dagger}s\,\delta_{\sigma\sigma'} = |s|^2\delta_{\sigma\sigma'},\tag{57}$$

which is only faithful when large-N is abandoned and  $|s|^2 = 1$ . Now since  $s^{\dagger}s$  commutes with s, we may normalize the algebra by writing

$$d_{\sigma}^{\dagger} = f_{\sigma}^{\dagger} \frac{s}{\sqrt{s^{\dagger}s}}.$$
 (58)

This restores the normalization of the canonical commutation relation  $\{d_{\sigma}, d_{\sigma'}^{\dagger}\} = \delta_{\sigma\sigma'}$ . By comparing (58) with (5), we identify the slave rotor phase with the phase of the s-boson:

$$s = \sqrt{s^{\dagger}s}e^{i\theta} \tag{59}$$

yielding the fundamental relation

$$e^{i\theta} = L_{+} = \frac{s}{\sqrt{s^{\dagger}s}},$$

$$s = b + t^{\dagger}.$$
(60)

Both representations successfully capture the lower and upper Hubard bands and central Kondo resonance features in the SIAM. We now demonstrate that when the large-N expansion is abandoned (taking N=2) in the s-boson approach and enforcing  $|s|^2=1$ , the s-boson and slave rotor approaches share a common action, thus unifying the two approaches. This constraint can be implemented by including an additional term  $\frac{U(h-1)}{4}$  ( $\bar{s}s-1$ ) in the action (28),

$$S = S_c + \int_0^\beta d\tau \left[ \frac{U}{4} \bar{s} \left( 1 - \frac{(\partial_\tau + \lambda - \tilde{\epsilon}_d)^2}{(U/2)^2} \right) s + \sum_\sigma f_\sigma^\dagger (\partial_\tau + \lambda) f_\sigma + V \sum_{\mathbf{k}\sigma} \left( c_{\mathbf{k}\sigma}^\dagger f_\sigma s + \text{H.c.} \right) + \frac{U(h(\tau) - 1)}{4} \left( \bar{s}\bar{s} - 1 \right) - \lambda Q \right]$$

$$= S_c + \int_0^\beta d\tau \left[ \frac{U}{4} \bar{s} \left( h(\tau) - \frac{(\partial_\tau + \lambda - \tilde{\epsilon}_d)^2}{(U/2)^2} \right) s + \sum_\sigma f_\sigma^\dagger (\partial_\tau + \lambda) f_\sigma + V \sum_{\mathbf{k}\sigma} \left( c_{\mathbf{k}\sigma}^\dagger f_\sigma s + \text{H.c.} \right) - \frac{Uh}{4} - \lambda Q \right], \tag{61}$$

where  $S_c$  is the conduction electron action that is bilinear in the grassman c, and the constraint  $\bar{s}s = |s|^2 = 1$  is policed by the Lagrange multiplier  $h(\tau)$ .

The O(2) rotor action from Florens and Georges [40],  $S_{\text{rotor}} = \int_0^\beta d\tau L_{\text{rotor}}$ , can be written by converting the slave rotor field  $e^{i\theta} \to X$  as a complex field X, where  $\theta(\tau)$  is the phase variable conjugate to the local impurity charge and the amplitude field X is subject to the constraint  $|X|^2 = 1$ . The rotor Lagrangian  $L_{\text{rotor}}$  is,

$$L_{\text{rotor}} = \sum_{\mathbf{k},\sigma} c_{\mathbf{k}\sigma}^{\dagger} (\partial_{\tau} + \epsilon_{\mathbf{k}}) c_{\mathbf{k}\sigma} + \sum_{\sigma} f_{\sigma}^{\dagger} (\partial_{\tau} + \epsilon_{d} - \lambda) f_{\sigma} + \tilde{h}(\tau) (|X|^{2} - 1)$$

$$+ \lambda Q - \frac{\lambda^{2}}{2U} |X|^{2} + \frac{|\partial_{\tau} X|^{2}}{2U} + \frac{\lambda}{2U} (\bar{X} \partial_{\tau} X - \text{h.c.}) + V_{0} \sum_{\mathbf{k}\sigma} (c_{\mathbf{k}\sigma}^{\dagger} f_{\sigma} X + \text{H.c.}),$$
(62)

where we have generalized the constraint to arbitrary filling Q rather than half-filling Q = N/2. Here, the dynamical field  $\tilde{h}$  imposes the constraint  $|X|^2 = 1$ . Note that unlike our starting model's hybridization (11), there is no  $\sqrt{N}$  in the denominator and the amplitude of the X field is constrained to be one,  $|X|^2 = 1$ , implemented by the Lagrange multiplier  $h(\tau)$ . Hence the terms bilinear in X boson operators are not  $\mathcal{O}(N)$  and thus the O(2) slave rotor does not have a controlled large-N expansion.

The rotor action can then be rewritten as (see Appendix F for details),

$$S_{\text{rotor}} = \int_{0}^{\beta} d\tau \left[ \sum_{\sigma} f_{\sigma}^{\dagger} \left( \partial_{\tau} + \lambda \right) f_{\sigma} + \frac{U}{8} \bar{X} \left( \frac{8}{U} \tilde{h} - \frac{\left( \partial_{\tau} + \lambda - \tilde{\epsilon}_{d} \right)^{2}}{(U/2)^{2}} \right) X + V_{0} \sum_{\mathbf{k}\sigma} \left( c_{\mathbf{k}\sigma}^{\dagger} f_{\sigma} \bar{X} + \text{H.c.} \right) - \tilde{h} - \lambda Q \right]$$
(63)

If we rescale  $X/\sqrt{2} \to X$ , relabel  $V = \sqrt{2}V_0$ , and  $h = 8\tilde{h}/U$ , then the rotor action (63) is identical to the normalized s-boson action (61) up to a discrepancy of a factor of two in the term Uh/8,

$$S_{\text{rotor}} = \int_{0}^{\beta} d\tau \left[ \sum_{\sigma} f_{\sigma}^{\dagger} \left( \partial_{\tau} + \lambda \right) f_{\sigma} + \frac{U}{4} \bar{X} \left( h - \frac{\left( \partial_{\tau} + \lambda - \tilde{\epsilon}_{d} \right)^{2}}{(U/2)^{2}} \right) X + V \sum_{\mathbf{k}\sigma} \left( c_{\mathbf{k}\sigma}^{\dagger} f_{\sigma} \bar{X} + \text{H.c.} \right) - \frac{Uh}{8} - \lambda Q \right]. \tag{64}$$

The identification of the slave rotor and the normalized s-boson SIAM actions allows for methodological advances. Writing the rotor action in a simpler s-boson form (64) allows for Gaussian fluctuations, akin to what was presented in Sec. II F, to be calculated simply. The generalization of the rotor constraint, inspired by connecting these actions, allows for accurate calculations around any chosen integer occupancy Q rather than only near half-filling (Q = N/2). However, our theory currently lacks a clear prescription for smoothly transitioning between integer occupancy sectors Q and  $Q \pm 1$ , requiring manual stepwise increases in Q, highlighting a challenge in describing the full mixed valence phase space as a function of filling within the parton framework.

The comparison between unnormalized s-boson and slave rotor/ normalized s-boson approaches reveals a fundamental dichotomy in the parton formalism. Parton methods must choose between a controlled large-N mean-field treatment and faithfulness to the physical d-electron anticommutation relation. Our s-boson method, like its antecedent, enables a controlled large-N expansion that correctly captures atomic energies but while it faithfully captures the rotor algebra, it intro-

duces a renormalization to the canonical commutation relations. Nevertheless, despite the imperfect algebra, the method successfully captures the essence of the physics including Coulomb blockade behavior and the formation and destruction of the Kondo resonance within a controlled mean-field framework. Conversely, slave rotor/normalized s-boson methods preserve algebraic structure through unitary transformations but lack tractable or accurate large N treatments. It is desirable for future analytical impurity solvers to be able to achieve both tractable large N mean-field treatment and algebraic faithfulness.

The unnormalized s-boson approach encounters difficulties in the strong mixed valence regime, where Q and  $Q \pm 1$  atomic configurations coexist. This manifests as a non-smooth interpolation of  $T_c$  at half-integer filling, where mixed valence is the strongest (Fig. 3). These limitations arise from the unfaithfully enlarged Hilbert space (Fig. 1) inherent in the parton formulation. While fictious states with a large number of b and t slave bosons are energetically suppressed by the large atomic excitation energies in the Kondo limit – where only physical  $Q \rightleftharpoons Q \pm 1$  functions remain low energy – they become

problematic in the strongly mixed valent regime. As either charge gap  $\Delta E_{\pm}$  approach zero, these fictitious states become degenerate with physical charge states, allowing the t and b slave boson occupation numbers to diverge. The normalization procedure of the s-boson may resolve this issue by projecting out nonphysical states, potentially enabling accurate description of strong mixed valence regimes where Hubbard bands merge with the central Kondo resonance.

Several extensions of our approach warrant future investigation. These include generalizations of the two pole structure of the s-boson to more complex atomic limits involving spin-orbit coupling and multiorbital physics

with intra-orbital, inter-orbital, and Hund's interactions. Further directions encompass systems with more complicated conduction bath density of states and hybridization functions, as well as applications to the periodic Anderson and Hubbard models.

#### ACKNOWLEDGMENTS

The authors are grateful for useful conversations with A. Gleis. This work was supported by the Office of Basic Energy Sciences, Material Sciences and Engineering Division, U.S. Department of Energy (DOE) under contract DE-FG02- 99ER45790 (L.L.H.L. and Pi.C.).

- A. Georges and G. Kotliar, Hubbard model in infinite dimensions, Phys. Rev. B 45, 6479 (1992).
- [2] A. Georges, G. Kotliar, W. Krauth, and M. J. Rozenberg, Dynamical mean-field theory of strongly correlated fermion systems and the limit of infinite dimensions, Rev. Mod. Phys. 68, 13 (1996).
- [3] G. Kotliar, S. Y. Savrasov, K. Haule, V. S. Oudovenko, O. Parcollet, and C. A. Marianetti, Electronic structure calculations with dynamical mean-field theory, Rev. Mod. Phys. 78, 865 (2006).
- [4] G. R. Stewart, Heavy-fermion systems, Rev. Mod. Phys. 56, 755 (1984).
- [5] P. A. Lee, T. M. Rice, J. W. Serene, L. J. Sham, and J. W. Wilkins, Theories of Heavy-Electron Systems, Comments Condens. Matt. Phys. 12, 99 (1986).
- [6] H. R. Ott, Heavy Electron Materials, in *Progress in Low Temp Physics*, Vol. 11, edited by D. F. Brewer (North Holland, Amsterdam, 1987) p. 215.
- [7] P. Fulde, J. Keller, and G. Zwicknagl, Theory of Heavy Fermion Systems, in *Solid State Physics*, Vol. 41, edited by H. Ehrenreich and D. Turnbull (Academic Press, 1988) pp. 1–150.
- [8] N. Grewe and F. Steglich, Heavy Fermions, in *Handbook on the Physics and Chemistry of Rare Earths*, Vol. 14, edited by K. A. Gschneider and L. Eyring (Elsevier, Amsterdam, 1991) p. 343.
- [9] P. Coleman, Heavy Fermions: Electrons at the Edge of Magnetism, Vol. 1 (Handbook of Magnetism and Advanced Magnetic Materials, John Wiley and Sons, Ltd., Hoboken, N.J., 2007) pp. 94–148.
- [10] D. Sherrington and P. Riseborough, Ionic Size Effects in Valence Transitions, Le Journal de Physique Colloques 37, C4 (1976), publisher: EDP Sciences.
- [11] P. S. Riseborough, Strong electron-phonon interactions in mixed valent states, Journal of Applied Physics 61, 3171 (1987).
- [12] A. C. Hewson and D. M. Newns, Polaronic effects in mixed and intermediate-valence compounds, Journal of Physics C: Solid State Physics 12, 1665 (1979).
- [13] A. C. Hewson and D. M. Newns, On the local polaron model and its applications to intermediate valence systems, J. Phys. C 13, 4477 (1980).
- [14] A. C. Hewson, A scaling approach to locally coupled electron-phonon systems, Journal of Physics C: Solid

- State Physics 14, 2747 (1981).
- [15] A. C. Hewson and D. Meyer, Numerical renormalization group study of the Anderson-Holstein impurity model, Journal of Physics: Condensed Matter 14, 427 (2001).
- [16] A. C. Hewson and J. Bauer, Numerical renormalization group study of probability distributions for local fluctuations in the Anderson-Holstein and Holstein-Hubbard models, Journal of Physics: Condensed Matter 22, 115602 (2010).
- [17] R. C. Monreal and A. Martin-Rodero, Equation of motion approach to the Anderson-Holstein Hamiltonian, Physical Review B 79, 115140 (2009), publisher: American Physical Society.
- [18] T. Hotta, Enhanced Kondo Effect in an Electron System Dynamically Coupled with Local Optical Phonon, Journal of the Physical Society of Japan 76, 084702 (2007), publisher: The Physical Society of Japan.
- [19] M. A. Laakso, D. M. Kennes, S. G. Jakobs, and V. Meden, Functional renormalization group study of the Anderson-Holstein model, New Journal of Physics 16, 023007 (2014), publisher: IOP Publishing.
- [20] E. Eidelstein, D. Goberman, and A. Schiller, Crossover from adiabatic to antiadiabatic phonon-assisted tunneling in single-molecule transistors, Phys. Rev. B 87, 075319 (2013).
- [21] L. L. H. Lau, A. Gleis, D. Kaplan, P. Chandra, and P. Coleman, Oscillate and renormalize: Fast phonons reshape the kondo effect in flat-band systems, Phys. Rev. B 111, 245149 (2025).
- [22] Z.-D. Song and B. A. Bernevig, MATBG as Topological Heavy Fermion: I. Exact Mapping and Correlated Insulators, arXiv:2111.05865 [cond-mat] (2021), arXiv:2111.05865 [cond-mat].
- [23] H. Shi and X. Dai, Heavy fermion representation for twisted bilayer graphene systems, Physical Review B 106, 245129 (2022).
- [24] D. Călugăru, M. Borovkov, L. L. H. Lau, P. Coleman, Z.-D. Song, and B. A. Bernevig, Twisted bilayer graphene as topological heavy fermion: II. Analytical approximations of the model parameters, Fiz. Nizk. Temp. 49, 703–719 (2023).
- [25] L. L. H. Lau and P. Coleman, Topological Mixed Valence Model for Twisted Bilayer Graphene, Phys. Rev. X 15, 021028 (2025).

- [26] Y.-Z. Chou and S. Das Sarma, Kondo lattice model in magic-angle twisted bilayer graphene, Phys. Rev. Lett. 131, 026501 (2023).
- [27] H. Hu, B. A. Bernevig, and A. M. Tsvelik, Kondo lattice model of magic-angle twisted-bilayer graphene: Hund's rule, local-moment fluctuations, and low-energy effective theory, Phys. Rev. Lett. 131, 026502 (2023).
- [28] H. Hu, G. Rai, L. Crippa, J. Herzog-Arbeitman, D. Călugăru, T. Wehling, G. Sangiovanni, R. Valentí, A. M. Tsvelik, and B. A. Bernevig, Symmetric kondo lattice states in doped strained twisted bilayer graphene, Phys. Rev. Lett. 131, 166501 (2023).
- [29] G. Rai, L. Crippa, D. Călugăru, H. Hu, F. Paoletti, L. de' Medici, A. Georges, B. A. Bernevig, R. Valentí, G. Sangiovanni, and T. Wehling, Dynamical correlations and order in magic-angle twisted bilayer graphene, Phys. Rev. X 14, 031045 (2024).
- [30] Li, Yantao and Fregoso, Benjamin M. and Dzero, Maxim, Topological mixed valence model in magic-angle twisted bilayer graphene, Phys. Rev. B 110, 045123 (2024).
- [31] J. Herzog-Arbeitman, J. Yu, D. Călugăru, H. Hu, N. Regnault, O. Vafek, J. Kang, and B. A. Bernevig, Heavy fermions as an efficient representation of atomistic strain and relaxation in twisted bilayer graphene (2025), arXiv:2405.13880 [cond-mat.mes-hall].
- [32] W. Zhao, B. Shen, Z. Tao, Z. Han, K. Kang, K. Watanabe, T. Taniguchi, K. F. Mak, and J. Shan, Gate-tunable heavy fermions in a moiré Kondo lattice, Nature 616,

- 61-65 (2023).
- [33] D. Guerci, J. Wang, J. Zang, J. Cano, J. H. Pixley, and A. Millis, Chiral Kondo lattice in doped MoTe<sub>2</sub>/WSe<sub>2</sub> bilayers, Science Advances 9, eade7701 (2023).
- [34] N. Andrei, K. Furuya, and J. H. Lowenstein, Solution of the kondo problem, Rev. Mod. Phys. 55, 331 (1983).
- [35] P. Coleman, New approach to the mixed-valence problem, Phys. Rev B29, 3035–3044 (1984).
- [36] N. Read and D. M. Newns, A new functional integral formalism for the degenerate Anderson model, J. Phys. C 29, L1055 (1983).
- [37] P. Coleman, Mixed Valence as an Almost Broken Symmetry, Phys. Rev. B 35, 5072 (1987).
- [38] J. Hubbard, Electron Correlations in Narrow Energy Bands. II. The Degenerate Band Case, Proc. R. Soc. London, Ser. A. 277, 237 (1964).
- [39] G. Kotliar and A. E. Ruckenstein, New functional integral approach to strongly correlated fermi systems: The gutzwiller approximation as a saddle point, Phys. Rev. Lett. 57, 1362 (1986).
- [40] S. Florens and A. Georges, Quantum impurity solvers using a slave rotor representation, Phys. Rev. B 66, 165111 (2002).
- [41] S. Florens and A. Georges, Slave-rotor mean-field theories of strongly correlated systems and the Mott transition in finite dimensions, Phys. Rev. B 70, 035114 (2004).

#### Appendix A: Calculation of the Effective Action

We start with the action for the SIAM with the physical d-electron represented as  $d_{\sigma}^{\dagger} \to f_{\sigma}^{\dagger} (b + t^{\dagger})$ , where  $f_{\sigma}^{\dagger}$  is a spinon operator and the two bosons b and t keep track of valence fluctuations,

$$S_A = \int_0^\beta d\tau \left[ f_\sigma^\dagger (\partial_\tau + \lambda) f_\sigma + \bar{b} (\partial_\tau + \Delta E_-^Q + \lambda) b + \bar{t} (\partial_\tau + \Delta E_+^Q - \lambda) t + \frac{V_0}{\sqrt{N}} \sum_{\mathbf{k}\sigma} \left( c_{\mathbf{k}\sigma}^\dagger f_\sigma \left( \bar{b} + t \right) + \text{h.c.} \right) - \lambda Q \right], \quad (A1)$$

where the atomic ionization energies are,

$$\Delta E_{+}^{Q} = E_{Q+1} - E_{Q} = \tilde{\epsilon}_{d} + U/2$$

$$\Delta E_{-}^{Q} = E_{Q-1} - E_{Q} = -\tilde{\epsilon}_{d} + U/2. \tag{A2}$$

where we have introduced the notation

$$\tilde{\epsilon}_d = \epsilon_d + U(Q - N/2) \tag{A3}$$

for the d-level position at doping away from half filling. We can write a symmetric s and antisymmetric a boson:

$$s = (b + \bar{t}), \quad a = (b - \bar{t}), \tag{A4}$$

such that the particle hole transformation acts as  $s \to \bar{s}$ , and  $a \to -\bar{a}$ .

$$S_{A} = \int_{0}^{\beta} d\tau \left[ f_{\sigma}^{\dagger} (\partial_{\tau} + \lambda) f_{\sigma} + \frac{1}{4} (\bar{s} + \bar{a}) (\partial_{\tau} - \tilde{\epsilon}_{d} + U/2 + \lambda) (s + a) + \frac{1}{4} (s - a) (\partial_{\tau} + \tilde{\epsilon}_{d} + U/2 - \lambda) (\bar{s} - \bar{a}) + \frac{V_{0}}{\sqrt{N}} \sum_{\mathbf{k}\sigma} \left( c_{\mathbf{k}\sigma}^{\dagger} f_{\sigma} \bar{s} + \text{h.c.} \right) - \lambda Q \right],$$
(A5)

We can commute  $\bar{t}t = t\bar{t}$ , which are just numbers, which flips of the sign for  $\partial_{\tau}$ , which can be seen more clearly in Matsubara frequency.

$$S_A = \int_0^\beta d\tau \left[ f_\sigma^\dagger (\partial_\tau + \lambda) f_\sigma + \frac{1}{4} (\bar{s} + \bar{a}) (\partial_\tau + U/2 + \lambda - \tilde{\epsilon}_d) (s + a) \right]$$

$$+ \frac{1}{4}(\bar{s} - \bar{a})(-\partial_{\tau} + U/2 - \lambda + \tilde{\epsilon}_d)(s - a) + \frac{V_0}{\sqrt{N}} \sum_{\mathbf{k}\sigma} \left(c_{\mathbf{k}\sigma}^{\dagger} f_{\sigma} \bar{s} + \text{h.c.}\right) - \lambda Q \right], \tag{A6}$$

Expanding,

$$S_{A} = \int_{0}^{\beta} d\tau \left[ f_{\sigma}^{\dagger} \left( \partial_{\tau} + \lambda \right) f_{\sigma} + \frac{U}{4} (\bar{s}s + \bar{a}a) + \frac{1}{2} \bar{s} \left( \partial_{\tau} + \lambda - \tilde{\epsilon}_{d} \right) a \right] + \frac{1}{2} \bar{a} \left( \partial_{\tau} + \lambda - \tilde{\epsilon}_{d} \right) s + \frac{V_{0}}{\sqrt{N}} \sum_{\mathbf{k}\sigma} \left( c_{\mathbf{k}\sigma}^{\dagger} f_{\sigma} \bar{s} + \text{h.c.} \right) - \lambda Q \right].$$
(A7)

Only the s boson couples to the fermions, so we can integrate out the a bosons to get,

$$S_{A} = \int_{0}^{\beta} d\tau \left[ \bar{f}_{\sigma} \left( \partial_{\tau} + \lambda \right) f_{\sigma} + \frac{1}{U} \bar{s} \left( \left( \frac{U}{2} \right)^{2} - (\partial_{\tau} + \lambda - \tilde{\epsilon}_{d})^{2} \right) s + \frac{V_{0}}{\sqrt{N}} \sum_{\mathbf{k}\sigma} \left( c_{\mathbf{k}\sigma}^{\dagger} f_{\sigma} \bar{s} + \text{H.c.} \right) - \lambda Q \right], \tag{A8}$$

#### Appendix B: Mean-Field Theory Analytical Results

We now present some analytical results for a single impurity Anderson model with a conduction sea with a constant density of states  $\rho$ . We will first derive the mean-field results using both the "top" t and "bottom" b bosons, before switching over to the more economical symmetric s boson.

Starting from the saddle-point of the action (A1), where  $b(\tau) = b$  and  $t(\tau) = t$  have no dynamics, integrating out the conduction band yields the following free energy,

$$F = -TN \sum_{|\omega_n| < D_c} \ln \left[ \lambda - i\omega_n + \frac{1}{N} \sum_{\mathbf{k}} \frac{V_0^2(\bar{b} + t)(b + \bar{t})}{i\omega_n - \epsilon_{\mathbf{k}}} \right] + (\Delta E_+^Q - \lambda) \, \bar{t}t + (\Delta E_-^Q + \lambda) \, \bar{b}b - \lambda Q, \tag{B1}$$

where  $D_c = \min(D, U/2)$ , the high-energy cutoff, depends on the relative size of the bandwidth D and the Coulomb interaction U. If we consider a conduction sea with a constant density of conduction states  $\rho$  with a band-width 2D, the mean-field free energy can be rewritten as,

$$F = -TN \sum_{|\omega_n| < D_c} \ln\left[\lambda - i\omega_n - i\tilde{\Delta}_n\right] e^{i\omega_n 0^+} + \left(\Delta E_+^Q - \lambda\right) \bar{t}t + \left(\Delta E_-^Q + \lambda\right) \bar{b}b - \lambda Q, \tag{B2}$$

where we have explicitly written out the convergence factor and the f-electron self energy due to the hybridization with the conduction sea can be approximated as,

$$\frac{1}{N} \sum_{\mathbf{k}} \frac{V_0^2(\bar{b} + t)(b + \bar{t})}{i\omega_n - \epsilon_{\mathbf{k}}} \approx -i\tilde{\Delta} \operatorname{sgn}(\omega_n), \tag{B3}$$

where the real part is negligible due to being  $\mathcal{O}(\omega_n/D)$  and taking the large bandwidth approximation. Here we define,  $\tilde{\Delta} = \pi \rho V_0^2 (\bar{b} + t)(b + \bar{t})/N = \Delta(\bar{b} + t)(b + \bar{t})$ , where  $\Delta$  is the bare hybridization width, and  $\tilde{\Delta}_n \equiv \tilde{\Delta} \operatorname{sgn}(\omega_n)$ . Carrying out the particle-hole transformation on the free energy,

$$F = -TN \sum_{|\omega_{n}| < D_{c}} \ln\left[-\lambda - i\omega_{n} - i\tilde{\Delta}_{n}\right] e^{i\omega_{n}0^{+}} + \left(\Delta E_{-}^{Q} + \lambda\right) \bar{b}b + \left(\Delta E_{+}^{Q} - \lambda\right) \bar{t}t - \lambda(Q - N)$$

$$= -TN \sum_{|\omega_{m}| < D_{c}} \ln\left[\lambda - i\omega_{m} - i\tilde{\Delta}_{m}\right] e^{-i\omega_{m}0^{+}} + \left(\Delta E_{-}^{Q} + \lambda\right) \bar{b}b + \left(\Delta E_{+}^{Q} - \lambda\right) \bar{t}t - \lambda(Q - N), \tag{B4}$$

where we have relabeled  $\omega_m = -\omega_n$ . Summing (B4) and (B2), we obtain,

$$F = -TN \sum_{|\omega_n| < D_c} \ln\left[\lambda - i\omega_n - i\tilde{\Delta}_n\right] \cos\left(\omega_n 0^+\right) + \left(\Delta E_+^Q - \lambda\right) \bar{t}t + \left(\Delta E_-^Q + \lambda\right) \bar{b}b - \lambda\left(Q - N/2\right), \tag{B5}$$

Introducing the complex d-level  $\xi = \lambda + i\tilde{\Delta}$ , then

$$\sum_{|\omega_n| < D_c} \ln \left[ \lambda - i\tilde{\Delta}_n - i\omega_n \right] \cos \left( \omega_n 0^+ \right) = 2 \operatorname{Re} \sum_{D_c > \omega_n > 0} \ln \left[ \xi + i\omega_n \right]$$

$$= 2\operatorname{Re} \sum_{n=0}^{M-1} \ln \left[ n + \frac{1}{2} + \frac{\xi}{2\pi i T} \right] + \operatorname{const}$$

$$= 2\operatorname{Re} \ln \left[ \prod_{n=0}^{M-1} \left( n + \frac{1}{2} + \frac{\xi}{2\pi i T} \right) \right] + \operatorname{const},$$
(B6)

where we have introduced  $M = D_c/(2\pi T)$ , and we will ignore the overall constant, proportional to  $\ln[2\pi iT]$  on the second line. Since the gamma function  $\Gamma(x)$  has the property  $\Gamma(1+x) = x\Gamma(x)$ , it follows that,

$$\prod_{n=0}^{M-1} (n+x)\Gamma(x) = \Gamma(M+x),\tag{B7}$$

so that

$$\prod_{n=0}^{M-1} (n+x) = \frac{\Gamma(M+x)}{\Gamma(x)}.$$
(B8)

Hence, we can rewrite,

$$\prod_{n=0}^{M-1} \left( n + \frac{1}{2} + \frac{\xi}{2\pi i T} \right) = \frac{\tilde{\Gamma}(\xi + iD_c)}{\tilde{\Gamma}(\xi)},\tag{B9}$$

where we have introduced the short-hand,

$$\tilde{\Gamma}(z) = \Gamma\left(\frac{1}{2} + \frac{z}{2\pi i T}\right). \tag{B10}$$

We can now rewrite the mean-field free energy (B2) in the compact form,

$$F = -2TN\operatorname{Re}\ln\left[\frac{\tilde{\Gamma}(\xi + iD_c)}{\tilde{\Gamma}(\xi)}\right] + (\Delta E_+^Q - \lambda)\,\bar{t}t + (\Delta E_-^Q + \lambda)\,\bar{b}b - \lambda\,(Q - N/2)$$

$$= N\operatorname{Re}\left(2T\ln\tilde{\Gamma}(\xi) - \frac{\xi}{i\pi}\ln\left[\frac{D_c}{2\pi T}\right]\right) + (\Delta E_+^Q)\,\bar{t}t + (\Delta E_-^Q)\,\bar{b}b - \lambda\,(Q - N/2)\,, \tag{B11}$$

where we have assumed  $\xi$  is small compared to  $D_c$  to taylor expand,

$$2T \ln \tilde{\Gamma}(\xi + iD_c) \approx 2T \ln \tilde{\Gamma}(iD_c) + \tilde{\psi}(iD_c) \frac{\xi}{i\pi}$$

$$\approx 2T \ln \tilde{\Gamma}(iD_c) + \frac{\xi}{i\pi} \ln \frac{D_c}{2\pi T}$$
(B12)

where we have denoted  $\tilde{\psi}(\xi) = \psi\left(\frac{1}{2} + \frac{\xi\beta}{2\pi i}\right)$ , and  $\psi(z) = \frac{\partial \ln\Gamma(z)}{\partial z}$  is the digamma function. The second line, we have assumed  $D_c/(2\pi T)$  is large and replaced the digamma function's asymptotic behavior with a logarithm,  $\psi(z) \to \ln z$  for large z.

The saddle-point equations can be found by differentiating with respect to  $\lambda$ , b, and t. First differentiating with respect to  $\lambda$ ,

$$\frac{\partial F}{\partial \lambda} = \frac{N}{\pi} \operatorname{Im} \left[ \tilde{\psi}(\xi) \right] + \bar{b}b - \bar{t}t - Q + N/2 = 0$$

$$= \frac{N}{\pi} \operatorname{Im} \left[ \tilde{\psi}(\xi) + \frac{i\pi}{2} \right] + \bar{b}b - \bar{t}t - Q = 0. \tag{B13}$$

Differentiating with respect to the two bosons yields,

$$\frac{\partial F}{\partial \bar{t}} = \frac{N\Delta(\bar{b}+t)}{\pi} \operatorname{Re}\left[\tilde{\psi}(\xi) - \ln\left(\frac{D_c}{2\pi T}\right)\right] + \left(\Delta E_+^Q - \lambda\right) t = 0,$$

$$\frac{\partial F}{\partial \bar{b}} = \frac{N\Delta(b+\bar{t})}{\pi} \operatorname{Re}\left[\tilde{\psi}(\xi) - \ln\left(\frac{D_c}{2\pi T}\right)\right] + \left(\Delta E_-^Q + \lambda\right) b = 0.$$
(B14)

We can hence see that we could have absorbed  $\lambda N/2$  into an additional i in the logarithm and rewritten the free energy as,

$$F = N \operatorname{Re} \left( 2T \ln \tilde{\Gamma}(\xi) - \frac{\xi}{i\pi} \ln \left[ \frac{D_c}{2\pi i T} \right] \right) + (\Delta E_+^Q) \, \bar{t}t + (\Delta E_-^Q) \, \bar{b}b - \lambda Q. \tag{B15}$$

Alternatively, the mean-field free energy can be derived using the saddle-point approximation for the action (A8) where the s-boson has no dynamics. Integrating out the conduction band yields,

$$F = -TN \sum_{\omega_n < D_c} \ln\left[\lambda - i\tilde{\Delta}_n - i\omega_n\right] + \frac{|s|^2 V_0^2}{J(\lambda)} - \lambda Q,$$
(B16)

where  $i\tilde{\Delta}_n = i\pi\rho V_0^2 |\tilde{s}|^2 \text{sgn}(n)$  is the large-cutoff approximation for the f-electron self energy, where  $\tilde{s} = s/\sqrt{N}$ . Lastly, the  $\lambda$ -dependent Kondo coupling has the Schrieffer-Wolff form,

$$J(\lambda) = \frac{V_0^2}{U/2 + \lambda - \tilde{\epsilon}_d} + \frac{V_0^2}{U/2 - \lambda + \tilde{\epsilon}_d}$$
(B17)

We can rewrite the free energy (B16),

$$F = N \operatorname{Re} \left( 2T \ln \tilde{\Gamma}(\xi) - \frac{\xi}{i\pi} \ln \left[ \frac{D_c}{2\pi i T} \right] \right) + \frac{|s|^2 V_0^2}{J(\lambda)} - \lambda Q$$
$$= N \operatorname{Im} \left[ 2iT \ln \tilde{\Gamma}(\xi) - \frac{\xi}{\pi} \ln \frac{D_c}{2\pi i T} \right] + \frac{|s|^2 V_0^2}{J(\lambda)} - \lambda Q. \tag{B18}$$

We can then rewrite,

$$\frac{|s|^2 V_0^2}{J(\lambda)} - \lambda Q = \frac{N \operatorname{Im}\left[\xi\right]}{\pi} \left[ \ln e^{\frac{1}{\rho J(\lambda)}} - \ln e^{i\pi q} \right], \tag{B19}$$

where q = Q/N. Hence the free energy is,

$$F = N \operatorname{Im} \left[ 2iT \ln \tilde{\Gamma}(\xi) - \frac{\xi}{\pi} \ln \frac{T_K(\lambda)e^{i\pi q}}{2\pi iT} \right] \equiv N \operatorname{Im} F_c , \qquad (B20)$$

where  $T_K(\lambda) = D_c \exp\left[-\frac{1}{\rho J(\lambda)}\right]$  is the  $\lambda$ -dependent Kondo temperature.

In the Kondo limit, we can neglect the  $\lambda$  dependence of the Kondo coupling constant, setting  $J = J(\lambda = 0)$ . In this limit In this limit, we obtain the saddle point equations by differentiating (B20) with respect to  $\xi$ . Setting  $\partial F_c/\delta \xi = 0$ , we obtain

$$\tilde{\psi}(\xi) = \ln\left(\frac{T_K e^{i\pi q}}{2\pi i T}\right),\tag{B21}$$

 $T_K = T_K(\lambda)|_{\lambda=0} = D_c \exp\left[-\frac{1}{\rho J}\right]$  is the Kondo temperature. At low temperature, we can approximate  $\tilde{\psi}(z) = \ln(\frac{z}{2\pi i T})$ , so we obtain simply  $\xi = \lambda + i\tilde{\Delta} = T_K e^{i\pi q}$ , recovering the large N limit of the SU(N) Kondo model, but with the finite U Schrieffer-Wolff form of the coupling constant J(B17).

For the fully mixed valence regime, the  $\lambda$  dependence in the Kondo coupling  $J(\lambda)$  cannot be ignored, and the saddle-point equations are obtained by minimizing (B18), replacing Eqs. (B13) and (B14),

$$\frac{\partial F}{\partial \lambda} = \frac{N}{\pi} \left( \operatorname{Im} \left[ \tilde{\psi}(\xi) - \ln \frac{D_c}{2\pi i T} \right] + 2 \frac{(\tilde{\epsilon}_d - \lambda)}{U} |\tilde{s}|^2 - q \right) = 0$$

$$= \frac{N}{\pi} \left( \operatorname{Im} \left[ \tilde{\psi}(\xi) + \frac{i\pi}{2} \right] + 2 \frac{(\tilde{\epsilon}_d - \lambda)}{U} |\tilde{s}|^2 - q \right) = 0$$

$$\frac{\partial F}{\partial \bar{s}} = sV_0^2 \rho \left( \operatorname{Re} \left[ \tilde{\psi}(\xi) - \ln \frac{T_K(\lambda)}{2\pi T} \right] \right) = 0, \tag{B22}$$

The two saddle-point equations can be written as a single complex equation,

$$\tilde{\psi}(\xi) - \ln\left(\frac{T_K(\lambda)e^{i\pi q}}{2\pi i T}\right) = -2\pi i \frac{\tilde{\epsilon}_d - \lambda}{U} |\tilde{s}|^2.$$
(B23)

## Appendix C: Gaussian Fluctuations in the Cartesian Gauge

The full expressions for the normal and anomalous Bose self energies are,

$$\Pi_{0}(i\nu_{m}) = \left(\frac{\Delta}{\pi} \left[\tilde{\psi}(\xi + i\nu_{m}) - \tilde{\psi}(\xi)\right]\right)^{*} + \left(\frac{2\tilde{\Delta}^{2}}{\nu_{n}(\nu_{n} + 2\tilde{\Delta})}\right) \frac{\Delta}{\pi} \operatorname{Re}\left[\tilde{\psi}(\xi + i\nu_{m}) - \tilde{\psi}(\xi)\right] + \frac{\Delta}{\pi} \operatorname{Re}\left[\tilde{\psi}(\xi) - \ln\frac{D}{2\pi i T}\right]$$

$$\Pi_{A}(i\nu_{m}) = \frac{2\tilde{\Delta}\left(\tilde{\Delta} + \nu_{m}\right)}{\nu_{m}(\nu_{m} + 2\tilde{\Delta})} \frac{\Delta}{\pi} \operatorname{Re}\left[\tilde{\psi}(\xi + i\nu_{m}) - \tilde{\psi}(\xi)\right],$$
(C1)

where the bare resonance width is  $\Delta = \pi \rho V_0^2/N$  and  $\rho$  is the constant conduction bath density of states at the Fermi level.  $\tilde{\Delta} = \Delta |\tilde{s}|^2$  is the renormalized resonance width when the s-boson gains a mean-field expectation value  $\tilde{s}$ . The Bose self-energies above are related to the corresponding susceptibilities by a negative sign. The complex d-level position is given by  $\xi = \lambda + i\tilde{\Delta} = \lambda$ , where the imaginary part vanishes because the renormalized hybridization width  $\tilde{\Delta} = \Delta |s|^2$  equals zero in the normal state when the s-boson has yet to develop a mean-field expectation value. In the normal boson state, the anomalous self energy  $\Pi_A(i\nu_m)$  and the central term in the normal self energy  $\Pi_0$  also both vanish.

#### Appendix D: Calculation of the Imaginary and Real Parts of the Physical d-electron Propagator

The full physical d-electron Green's function is defined as,

$$G_{d}(\tau) = -\langle \mathcal{T}d_{\sigma}(\tau)d_{\sigma}^{\dagger}(0)\rangle = -\langle \mathcal{T}s^{\dagger}(\tau)f_{\sigma}(\tau)f_{\sigma}^{\dagger}(0)s(0)\rangle$$

$$\approx -\langle \mathcal{T}f_{\sigma}(\tau)f_{\sigma}^{\dagger}(0)\rangle\langle s^{\dagger}(\tau)s(0)\rangle$$

$$= -G_{f}(\tau)D_{s}(-\tau). \tag{D1}$$

The full physical d-electron propagator is the Fourier transform of (D1),

$$G_{d}(i\omega_{n}) = \frac{1}{\beta} \int_{0}^{\beta} d\tau G_{d}(\tau) e^{i\omega_{n}\tau}$$

$$= -\frac{1}{\beta} \int_{0}^{\beta} d\tau \sum_{i\nu_{m}} \sum_{i\omega'_{l}} G_{f}(i\omega'_{l}) D_{s}(i\nu_{m}) e^{\tau(i\omega_{n}-i\omega'_{l}+i\nu_{m})}$$

$$= -\frac{1}{\beta} \sum_{i\nu_{m}} G_{f}(i\omega_{n}+i\nu_{m}) D_{s}(i\nu_{m}). \tag{D2}$$

Performing the bosonic matsubara sum on the complex plane,

$$G_d(i\omega_n) = \oint \frac{dz \, n_B(z)}{2\pi i} G_f(i\omega_n + z) D_s(z)$$

$$= \int \frac{dv}{\pi} D_s''(v - i\delta) \left[ \frac{n_B(v) + q}{i\omega_n - \lambda + v} \right], \tag{D3}$$

the real frequency local spectral function is then,

$$A_d(\omega) = \frac{1}{\pi} D_s''(\lambda - \omega) \left[ n_B(\lambda - \omega) + q \right]$$
 (D4)

# Appendix E: Charge Susceptibility Calculation in the Normal State

Including the Gaussian fluctuations into the constraint (17) describes the filling expectation of the d-electron,

$$\langle n_d(\tau) \rangle = \langle n_f(\tau) \rangle = Q + \frac{2}{U} \left\{ \Lambda \bar{s}(\tau) s(\tau) + \frac{1}{2} \left( \bar{s}(\tau) \partial_{\tau} [s(\tau)] - \partial_{\tau} [\bar{s}(\tau)] s(\tau) \right) \right\}, \tag{E1}$$

where  $\Lambda = \lambda - \tilde{\epsilon}_d$  and the second term on the right hand side describes the departure from integer valence Q. Hence the fluctuations of the d-electron occupancy in the normal phase when the boson has yet to condense is,

$$\delta n_d(\tau) = \frac{2}{U} \left\{ \Lambda \bar{s}(\tau) s(\tau) + \frac{1}{2} \left( \bar{s}(\tau) \partial_{\tau} [s(\tau)] - \partial_{\tau} [\bar{s}(\tau)] s(\tau) \right) \right\}, \tag{E2}$$

where we implicitly write  $s(\tau)$  as the fluctuation for brevity. The charge susceptibility in matsubara frequency  $\chi_c(i\nu_m) = \langle \delta n_d(-i\nu_m)\delta n_d(i\nu_m) \rangle$  can be calculated using the s-boson bubble with the vertex  $v_l = 2(\Lambda - i\omega_l - i\nu_m/2)/U$ ,

$$\chi_c(i\nu_m) = \frac{4T}{U^2} \sum_{i\omega_l} D_s(i\nu_m + i\omega_l) D_s(i\omega_l) \left[\Lambda - i\omega_l - i\nu_m/2\right]^2$$
 (E3)

With real frequency  $\nu$ ,

$$\chi_c(\nu - i\delta) = \frac{4}{U^2} \int_{-\infty}^{\infty} \frac{d\omega}{\pi} \int_{-\infty}^{\infty} \frac{d\omega'}{\pi} \frac{n_B(\omega) - n_B(\omega')}{\nu - i\delta + \omega - \omega'} D_s''(\omega') D_s''(\omega) \left[\Lambda - \left(\frac{\omega'}{2} + \frac{\omega}{2}\right)\right]^2.$$
 (E4)

So the imaginary part of the charge susceptibility is

$$\chi_c''(\nu) = \frac{4}{U^2} \int_{-\infty}^{\infty} \frac{d\omega}{\pi} \left( n_B(\omega) - n_B(\omega + \nu) \right) D_s''(\nu + \omega) D_s''(\omega) \left[ -\left(\frac{\nu}{2} + \omega\right) + \Lambda \right]^2.$$
 (E5)

## Appendix F: Connecting the s-Boson and Slave Rotor Actions

In this section we show that the slave rotor representation of the SIAM action can be transformed into a form that can be identified with the s-boson action where the s-boson is normalized such that  $\bar{s}s = |s|^2 = 1$ . Let us start from the sigma model Lagrangian for the slave rotor representation of the SIAM as written by Florens and Georges [40],

$$L_{\text{rotor}} = \sum_{\mathbf{k},\sigma} c_{\mathbf{k}\sigma}^{\dagger} (\partial_{\tau} + \epsilon_{\mathbf{k}}) c_{\mathbf{k}\sigma} + \sum_{\sigma} f_{\sigma}^{\dagger} (\partial_{\tau} + \tilde{\epsilon}_{d} - \lambda) f_{\sigma} + \tilde{h}(\tau) (|X|^{2} - 1)$$

$$+ \lambda \frac{N}{2} - \frac{\lambda^{2}}{2U} |X|^{2} + \frac{|\partial_{\tau} X|^{2}}{2U} + \frac{\lambda}{2U} (\bar{X} \partial_{\tau} X - \text{h.c.}) + V_{0} \sum_{\mathbf{k}\sigma} (c_{\mathbf{k}\sigma}^{\dagger} f_{\sigma} X + \text{H.c.}),$$
(F1)

where  $X = e^{i\theta}$  is the complex bosonic sigma-model field. Note that unlike our starting model's hybridization (11), there is no  $\sqrt{N}$  in the denominator, where the X field must constrained to be of order unity,  $|X|^2 = 1$ , implemented by the Lagrange multiplier  $\tilde{h}(\tau)$ . We can generalize the constraint to arbitrary filling Q rather than half-filling Q = N/2,

$$L_{\text{rotor}} = \sum_{\mathbf{k},\sigma} c_{\mathbf{k}\sigma}^{\dagger} (\partial_{\tau} + \epsilon_{\mathbf{k}}) c_{\mathbf{k}\sigma} + \sum_{\sigma} f_{\sigma}^{\dagger} (\partial_{\tau} + \tilde{\epsilon}_{d} - \lambda) f_{\sigma} + \tilde{h}(\tau) (|X|^{2} - 1)$$

$$+ \lambda Q - \frac{\lambda^{2}}{2U} |X|^{2} + \frac{|\partial_{\tau} X|^{2}}{2U} + \frac{\lambda}{2U} (\bar{X} \partial_{\tau} X - \text{h.c.}) + V_{0} \sum_{\mathbf{k}\sigma} (c_{\mathbf{k}\sigma}^{\dagger} f_{\sigma} X + \text{H.c.}),$$
(F2)

We first relabel  $\lambda \to -\lambda$ , and shift  $\lambda \to \lambda - \tilde{\epsilon}_d$ . Using the following two identities which discard nondynamical constants,

$$-\int_0^\beta d\tau \ \bar{X}\partial_\tau^2 X = \int_0^\beta d\tau \ |\partial_\tau X|^2, \quad \int_0^\beta d\tau \ \bar{X}\partial_\tau X = -\int_0^\beta d\tau \ \partial_\tau [\bar{X}] X,$$

(F1) can be rewritten as,

$$L_{\text{rotor}} = L_c + \sum_{\sigma} f_{\sigma}^{\dagger} (\partial_{\tau} + \lambda) f_{\sigma} + \tilde{h}(\tau) (|X|^2 - 1) + V_0 \sum_{\mathbf{k}\sigma} (c_{\mathbf{k}\sigma}^{\dagger} f_{\sigma} X + \text{H.c.})$$

$$- \frac{(\lambda - \tilde{\epsilon}_d) N}{2} - \frac{(\lambda - \tilde{\epsilon}_d)^2}{2U} |X|^2 - \frac{\bar{X} \partial_{\tau}^2 X}{2U} - \frac{(\lambda - \tilde{\epsilon}_d)}{U} \bar{X} \partial_{\tau} X, \tag{F3}$$

where  $L_c = \sum_{\mathbf{k},\sigma} c_{\mathbf{k}\sigma}^{\dagger} (\partial_{\tau} + \epsilon_{\mathbf{k}}) c_{\mathbf{k}\sigma}$ . Factoring terms,

$$L_{\text{rotor}} = L_c + \sum_{\sigma} f_{\sigma}^{\dagger} \left( \partial_{\tau} + \lambda \right) f_{\sigma} + \frac{U}{8} \bar{X} \left( \frac{8}{U} \tilde{h} - \frac{\left( \partial_{\tau} + \lambda - \tilde{\epsilon}_d \right)^2}{(U/2)^2} \right) X + V_0 \sum_{\mathbf{k}\sigma} \left( c_{\mathbf{k}\sigma}^{\dagger} f_{\sigma} \bar{X} + \text{H.c.} \right) - \tilde{h} - \lambda Q.$$
 (F4)

ı